



Electroless Copper Deposition Using Sn/Ag Catalyst on Epoxy Laminates

Erdal Uzunlar,* Zachary Wilson, and Paul A. Kohl**,^z

School of Chemical and Biomolecular Engineering, Georgia Institute of Technology, Atlanta, Georgia 30332-0100, USA

Electroless copper deposition was investigated on epoxy laminate substrates (Isola 185HR) using a silver-based catalyst, and a non-roughening surface treatment method based on sulfuric acid. The current challenges in electroless copper deposition include (i) high cost of Pd-based catalysts, (ii) deterioration of electrical performance of deposited metal at high frequency due to electron scattering at the roughened surface, and (iii) limited adhesion strength of electroless layers to substrates. We investigated an electroless copper deposition procedure composed of a H_2SO_4 surface pretreatment, two-step Sn/Ag nano-colloidal catalyst seeding, and immersion in a traditional formaldehyde-containing electroless copper bath. The H_2SO_4 pretreatment activated the epoxy surface for electroless deposition. Other strong acids did not lead to deposition. The H_2SO_4 treatment cleaned the substrate and provided the adhesion of the catalyst and electroless copper without increasing the surface roughness. XPS results showed a decrease in the carbonyl groups ($\text{C}=\text{O}$), and acid/ester functionalities ($\text{O}-\text{C}=\text{O}$) at the surface. Adsorbed sulfate on the substrate from the H_2SO_4 treatment led to Sn(II) sensitization. The tin-silver activation step resulted in Sn(IV) and Ag(0) products in the form of a Sn/Ag nano-colloidal catalyst. The Sn/Ag colloid acted as a catalyst for electroless copper deposition on the epoxy laminate substrates.

© 2013 The Electrochemical Society. [DOI: 10.1149/2.039312jes] All rights reserved.

Manuscript submitted September 30, 2013; revised manuscript received November 11, 2013. Published November 23, 2013. This was Paper 2355 from the San Francisco, California, Meeting of the Society, October 27–November 1, 2013. *This paper is part of the JES Focus Issue on Electrochemical Processing for Interconnects.*

The electroless deposition of copper is used in fabricating epoxy-based substrates for microelectronic devices, such as printed wiring boards (PWB).¹ The electroless copper layer can be utilized as a seed layer of electroplating (i.e. semi-additive process), or can be deposited to full metal thickness (i.e. fully additive process). The major challenges facing electroless deposition for interconnect include cost, deposition time, reliability, electrical conductivity, and excess surface roughness.¹⁻⁴ The insulating surface onto which the deposit to be made needs to be first catalytically activated prior to electroless copper deposition. The conventional Pd-based catalyst is expensive, due to the high cost of Pd.⁴ Another concern is the reliability of the deposit if there is poor adhesion between the deposited electroless copper layer and the substrate.^{2,3} In addition, the electrical performance of copper interconnect is adversely affected by surface roughness which results in surface scattering of electrons, especially at high frequency.⁴⁻⁶ At high frequency, the metal conductivity can be compromised because the conventional swell & etch process is based on an increase in the surface roughness in order to achieve acceptable adhesion through mechanical anchoring of the catalyst and the deposited metal.^{4,7,8} Thus, there is a need for improved catalysts which can lower the cost (i.e. non-palladium catalysts), and surface treatment methods which can avoid adding surface roughness (i.e. elimination of the swell & etch process).

The catalytic activity of the electroless copper deposition process is directly related to the oxidation of the reducing agent in the electroless bath, which is the rate-determining step in the process.³ The role of the surface catalyst is to facilitate the dissociative adsorption of the reducing agent (i.e. formaldehyde in this case) resulting in an adsorbed anion radical and adsorbed atomic hydrogen. The oxidation of adsorbed anion radical generates an electron, and the adsorbed atomic hydrogen recombines or becomes ionized.⁹ The established catalyst for electroless copper deposition is the Sn/Pd nano-colloid, which is highly effective at catalyzing the oxidation of formaldehyde.^{3,10} Holderer et al. previously showed that Sn/Pd is in a core-shell nano-particle form where the core is a Pd-Sn alloy with 60–70% Pd surrounded by a Sn shell.¹¹ The Sn/Pd nano-colloids are stabilized by SnCl_3^- complexes on the surface to prevent agglomeration.^{11,12} The dominance of the Pd-based catalyst is due to its high catalytic activity for oxidation of

a wide variety of reducing agents, and its stability and resistance to dissolution in the electroless bath.^{3,10,13,14} However, the high cost of Pd is an issue. In the seminal paper by Ohno et al., the catalytic activity of metallic Ag for formaldehyde oxidation was shown to be similar to Pd.⁹ Vaskelis et al. showed that Ag-based catalysts for electroless copper deposition can be formed by reducing Ag(I) to Ag(0) by Sn(II) oxidation to Sn(IV), a process similar to the conventional Sn/Pd colloidal catalyst formation.¹⁴ X-ray diffraction (XRD) measurements showed that the Sn/Ag nano-colloids had Ag in the metallic phase only, and Sn(IV) oxy-compounds, such as SnO_2 , which was speculated to give the nano-colloid a “self-stabilizing” property. Fujiwara et al. followed a similar procedure to prepare Sn/Ag nano-colloids, and used XRD to confirm that the nano-colloids had Ag core and SnO_2 shell.¹⁵ In addition, zeta potential measurements indicated the Ag/Sn nano-colloids were negatively charged because of an adsorbed Sn(IV) citrate layer on the nano-colloid surface providing the stability. Cationic surfactants were shown to adhere to the bare epoxy substrate and increase the density of adsorbed Ag nano-particles due to electrostatic interactions between the positively charged cationic surfactant on the substrate and the negatively charged Sn/Ag nano-colloid.¹⁶ In both studies,^{14,16} the catalytic activity of the Sn/Ag nano-colloids for electroless copper deposition was shown by cyclic voltammetry.

The adhesion strength of electroless copper layers onto PWBs is important in achieving reliable components. The adhesion strength of electroless copper to epoxy laminates (e.g. PWB) has been shown to have two contributions: mechanical adhesion and chemical adhesion.^{7,8,17-21} Mechanical adhesion is based on the increase of the surface in surface area due to roughness from micropores, cavities and asperities on the substrate surface.^{8,18,21} Generally, the higher the surface roughness, the higher the adhesion strength. The higher surface roughness leads to greater contact area between the epoxy laminate substrate and the metal as well as the catalyst.^{7,8,17,22,23} In addition, the presence of micropores and cavities creates mechanical interlocking between the epoxy laminate substrate and the catalyst/metal surface.^{8,22,24} Depositing the electroless copper in the micropores and cavities causes the epoxy failures to be cohesive in nature rather than adhesive. That is, the epoxy surrounding the pores fails cohesively during adhesion testing, rather than simply pulling the copper metal off the epoxy surface. On the other hand, chemical adhesion is based on the chemical affinity between the substrate surface and the catalyst/deposited metal.^{7,21,25} Chemical adhesion involves forming primary bonds, such as ionic or covalent bonds, at the epoxy/metal

*Electrochemical Society Student Member.

**Electrochemical Society Fellow.

^zE-mail: kohl@gatech.edu

interface.^{4,8,18,26} The type and the abundance of chemical functionalities on the substrate surface play a major role in the chemical adhesion.^{8,23,27} Chemical adhesion can be characterized by obtaining the density of functional groups on the surface and the oxygen-to-carbon ratio using X-ray photoelectron spectroscopy (XPS). Mechanical adhesion can be characterized by surface roughness measurements using atomic force microscopy (AFM).¹⁷ While both mechanisms contribute to total adhesion strength of the deposited metal, the mechanical adhesion is usually greater than the chemical adhesion.^{4,8,22,23,28} At high frequency, high surface roughness degrades the electrical signal due to electron scattering, especially when the surface roughness is comparable to the skin of the metal at the operating frequency.⁴⁻⁶ Thus, it is desirable to increase the chemical adhesion and minimize the surface roughness.

Surface pretreatment methods play an important role in the adhesion of electroless copper to insulating surfaces, such as PWBs. The surface pretreatment method cleans the substrate surface off impurities that can hinder the electroless deposition process, and mechanically and/or chemically conditions the surface for attachment of the catalyst.^{24,27} A number of surface pretreatments have been used to improve the adhesion of electroless copper to epoxy laminate substrates including wet-chemical treatments,^{7,8,24,25,28} surface modification through synthesis,^{20,21,29-31} plasma treatments,^{23,27} sonochemical treatments,^{32,33} photocatalytic reaction,³⁴ and treatment with surfactants.¹⁶ Two general categories of surface pretreatment are wet-chemical treatment and plasma treatment.^{7,17,23,27,35} Wet-chemical treatment is usually easy to implement and does not require expensive vacuum tools. The most common wet-chemical pretreatment for epoxy is the swell-and-etch process.^{4,17,24} The swell-and-etch process is based on increasing the surface roughness leading to high adhesion strength of the electrolessly deposited metal.^{7,8,17,21,24} The epoxy laminate has polar groups, such as primary and secondary alcohols and ethers, which are susceptible to oxidation.^{7,8,21} During swelling, the solvent (e.g. 2-(2-butoxyethoxy)ethanol) diffuses into the near-surface free volume of the epoxy causing swelling. The polymer chains are distorted in a way that exposes the polar groups to the epoxy surface, and creates channels into the epoxy which are lined with polar groups.^{7,8,17} During etching, an oxidizer (e.g. alkaline KMnO_4) oxidizes the polar groups and forms functionalities such as carboxylic acid, ketones, and aromatic alcohols, and breaks ether bonds in the epoxy, creating micropores and cavities.^{7,21,36} Although the effect of the oxidizer is isotropic in nature, the heterogeneous distribution of polar groups on the epoxy surface and within the near-surface region leads to different etch rates at the various sites. The etch rate is higher in regions where there is a high concentration of polar groups which leads to an increase in surface roughness.³⁵ In the swell-and-etch process, the physical anchoring contribution to the adhesion strength due to the high surface roughness is about 5 to 10 times greater than the chemical contribution to adhesion coming from the interaction of the catalyst and deposited copper with the oxidized functionalities on the epoxy laminate.²⁴

A second wet-chemical surface treatment method is chromic acid etching, which is less commonly used. Chromic acid etching is also based on an increase in surface roughness created by chemical etching with a strong oxidizer (e.g. $\text{K}_2\text{Cr}_2\text{O}_7$ in H_2SO_4).^{4,7,37,38} However, the increase in the surface roughness of an epoxy laminate is less than that for the swell-and-etch method.⁷ In addition, the hexavalent chromium is toxic, carcinogenic and corrosive.³⁹

The high frequency signal degradation that occurs in the roughened electroless copper layer is a performance issue for electronic devices. The surface roughness as a result of the conventional swell-and-etch process leads to high conductor losses in electroless copper on epoxy laminate substrates. In order to mitigate the signal loss, one approach is to use an electroless copper surface treatment that promotes chemical adhesion without increasing the surface roughness. The surface treatment method can utilize the already present surface roughness of the epoxy laminate to provide some mechanical adhesion anchoring. The chemical effect of the surface treatment method can modify the type and abundance of certain chemical functionalities so as to in-

crease the interfacial forces between the substrate, catalyst, and electroless copper. In a previous study, it was shown that a combined oxygen plasma treatment and hot sulfuric acid treatment produced adherent electroless layers deposited with a Sn/Ag catalysts on polyhedral oligomeric silsesquioxane (POSS) coated, smooth FR-4 boards.⁴ The role of oxygen plasma was to remove the organic component of the POSS. It is possible that the hot H_2SO_4 treatment increased the chemical adhesion on the smooth surface. Based on this result, the role of a H_2SO_4 treatment for epoxy surfaces was investigated as an alternative surface treatment to the swell-and-etch method in this study.

The goal of this study is to improve the electroless copper deposition process on epoxy laminate substrates using a non-palladium catalyst, and without the use of the swell-and-etch process. The motivation behind this study is three-fold: (i) there is a cost barrier with the conventional Pd-based catalysts in electroless deposition, (ii) the adhesion strength of the deposited electroless copper layer is critical to reliability, and (iii) the electrical performance of the deposited electroless copper is adversely affected by the surface roughness increase on which the conventional surface treatment methods are based (e.g. swell-and-etch method). Thus, it is attractive to lower the catalyst cost (i.e. non-palladium catalysts), and/or develop surface treatment methods that avoid adding surface roughness (i.e. elimination of the swell-and-etch process), without sacrificing the adhesion strength of the electrolessly deposited copper layers. In this study, different wet-chemical surface treatment methods including H_2SO_4 , H_3PO_4 and HCl treatments were investigated. The previously reported two-step catalyst seeding method involving Sn(II) oxidation to Sn(IV), and Ag(I) reduction to Ag(0) was used to activate the epoxy laminate surface for electroless copper.⁴ The Sn/Ag catalysts created by the process were characterized using X-ray photoelectron spectroscopy (XPS). The adhesion strength of the electroless copper layers was evaluated.

Experimental

Isola 185HR unclad laminate PWBs (Isola Global)⁴⁰ were used in this study. The standard surface treatment method used here was a hot H_2SO_4 treatment. The substrates were immersed in 12 M H_2SO_4 at 95°C for 30 min prior to Sn/Ag catalyst seeding. The electroless copper activation and plating process involved immersion in three sequential baths: (i) tin sensitization bath, (ii) silver activation bath, and (iii) electroless copper deposition bath, as outlined previously.^{4,41} The tin sensitization bath consisted of 1.4 g $\text{SnCl}_2 \cdot 2\text{H}_2\text{O}$, 2 mL HCl and 200 mL deionized (DI) H_2O . The tin sensitization was performed at 25°C for 30 min. The samples were then rinsed thoroughly with DI H_2O . The samples were then immersed in the silver activation bath which consisted of 0.75 g AgNO_3 , 10 g $(\text{NH}_4)_2\text{SO}_4$, 20 mL NH_4OH , and 180 mL H_2O . The silver activation was done at 25°C for 1 min, and the samples were then rinsed thoroughly with DI H_2O . The electroless copper deposition bath was composed of 0.75 g $\text{CuSO}_4 \cdot 5\text{H}_2\text{O}$ as the copper source, 1.89 g ethylenediaminetetraacetic acid (EDTA) as the complexing agent, 2.58 g potassium hydroxide for adjusting the pH, 0.2 mL Triton X-100 as the surfactant, 0.58 g paraformaldehyde $(\text{CH}_2\text{O})_n$ as the reducing agent and 200 mL DI H_2O . It is important that the components were added into the DI water in the order listed and given sufficient time to dissolve before the next component was added. The pH of the electroplating bath was measured to be 12.5. The electroless copper deposition was performed at 55°C for different deposition times. The deposition time was longer than the 3 min induction period of the electroless copper.⁴²

Several surface treatment methods were investigated for comparison with hot H_2SO_4 pretreatment in the default electroless copper process described above. These methods involve surface pretreatment using hot H_3PO_4 or HCl solutions. For consistency, the concentrations of H_3PO_4 and HCl were the same as that of H_2SO_4 , 12 M. The duration of the surface pretreatment was 30 min in each acid solution. The temperature for the H_3PO_4 treatment was kept constant at 95°C, whereas the temperature for HCl was kept constant at its boiling point at 48°C. For comparison of introduced surface roughness,

surface treatment using swell-and-etch method was also performed. The swelling step of the swell-and-etch process consisted of a 1:1 volume mixture of 2-(2-butoxyethoxy)ethanol and deionized (DI) water. The etching bath consisted of 55 g/L KMnO_4 and 1.2 M NaOH in DI water. First, a sample was washed under DI water followed by swelling for 7.5 minutes at 80°C . After swelling, the sample was rinsed with DI water, and then placed in the etching bath for 10 minutes at 80°C .⁷

The deposition rate of the electroless copper was obtained gravimetrically using a balance (Mettler AE200). Multiple samples were simultaneously processed in the sulfuric acid, tin sensitization, silver activation, and electroless copper baths. The samples for each electroless deposition time were taken out of the electroless copper bath, rinsed and blow-dried with dry N_2 . The mass of each sample after electroless copper deposition was measured. The electroless copper was then chemically stripped off the sample by immersion in concentrated HNO_3 for 3 to 5 s. Afterwards, the sample was rinsed with DI water, dried with nitrogen gas, and its mass was measured again. The difference between the two mass readings gave the amount of the electroless copper deposited. The superficial area of the each sample was used to calculate the deposition rate per unit area using the bulk density of copper.

The adhesion strength of the electrolessly deposited copper layer was evaluated by performing qualitative tape tests and quantitative pull tests. The thickness of the electrolessly deposited copper was increased in order to perform the quantitative adhesion strength tests. Copper was electroplated on the electroless copper using an acidic copper electroplating bath.⁴³ The recipe consisted of 200 g $\text{CuSO}_4 \cdot 5\text{H}_2\text{O}$, 60 g H_2SO_4 , 0.5 g polyethylene glycol (PEG), and 0.14 g CuCl in 1 L DI water. Copper was plated at a current density of 25 mA/cm^2 at room temperature for 50 to 60 min. The 90° peel test was then performed to quantify the adhesion strength of the electroless copper layer using an Instron load frame tool (Model 5842) following the ASTM B 533–85 standard. The test involved vertically peeling a 3-mm wide copper strip from the substrate surface. The pull force was measured as a function of time. The average pull force was divided by the width of the copper strip to give the peel strength in N/mm. At least three samples were run and acquired data were averaged to obtain each data point. The error range in 95% confidence interval for each data point was calculated.

The topography of the samples was investigated using a Veeco Dimension 3100 atomic force microscopy (AFM) with a Series 15 MikroMash single cantilever probe. A square area of $50 \times 50 \mu\text{m}$ was scanned for every measurement. The surface roughness measurements were done in tapping mode with a tip velocity of $25 \mu\text{m/s}$. The resolution of the scans was either 256 samples/line or 768 samples/line. In all measurements, the resonant frequency of the tip was constant at ca. 318.694 kHz, and the same proportional-integral control and amplitude set point parameters were used. The average (R_a) and root-mean-square (R_q) roughness values were extracted from the acquired AFM images using NanoScope Analysis v1.40 software. No smoothing of the images or data was applied. At least two measurements were performed for each sample, and the surface roughness was reported for the one with the larger surface roughness.

A second, quick turn-around surface topology characterization was performed in some experiments using a Dektak 3 profilometer. Individual line scans were obtained, and the average surface roughness was evaluated. The PWB surface was sometimes polished using a Buehler polisher with short felt pads (Carbimet 600/P1200) in order to decrease the surface roughness of the as-received PWBs without changing their materials. After polishing, the samples were rinsed with DI water, and blow-dried with N_2 . Three 1-mm Dektak line scans were obtained and averaged (i.e. average R_a and R_q values) for each sample. The samples then underwent surface pretreatment with H_2SO_4 , catalyst seeding (tin sensitization and silver activation), and electroless copper deposition.

The surface characterization of the samples was performed using a Thermo K-alpha X-ray photoelectron spectrometer (XPS). The energy step size of the survey scans was either 0.5 eV or 1 eV, whereas the energy step size for the elemental scans was 0.1 eV. The X-ray spot size

was $200 \mu\text{m}$ in diameter for all measurements. A low-voltage electron flood gun was kept on during measurements for charge compensation. In order to reduce noise in the XPS signals, each point was investigated twice for the survey scan, and five times for the elemental scan. The surface scans were performed without argon ion etching, whereas the atomic concentrations in the depth profiles were obtained using an argon ion gun with a raster size of 0.3 mm. The argon ion gun was operated with an ion energy of 3000 eV, and the current was adjusted to give an etch rate of 16.36 nm/s, as referenced to tantalum etching. The acquired XPS survey scans were analyzed using Avantage software.⁴⁴ The C1s signal was used as a reference signal for charge-shifting the acquired survey spectra so that the C1s peak position would be at 285.0 eV. In addition to the survey scans, high resolution elemental XPS scans were also performed. The elemental scans were used to confirm the presence of elements detected in survey scan results. The elemental scans were also used for detailed chemical characterization via deconvolution of individual peaks, such as the C1s peaks, into several peaks for that element corresponding to different oxidation states. The fractional composition for each oxidation state obtained from the deconvoluted spectra corresponds to their relative molar concentration on the substrate. The deconvolution and analysis of C1s signals were done using CasaXPS software.⁴⁵ The functional groups associated with the C1s scans were hydrocarbon functionalities C-C and C-H with reference peak position of 285.0 eV, alcohol and ether functionalities C-O-H and C-O-C with reference peak position of 286.5 eV, carbonyl functionality C=O with reference peak position of 288.0 eV, acid and ester functionalities O-C=O with reference peak position of 289 eV, and carbonate functionality O-C(=O)-O with reference peak position of 290.3 eV. The peak position tolerances were accepted as $\pm 0.2 \text{ eV}$ for all functional groups in the C1s spectra.⁴⁶ The full width at half maximum (fwhm) values for all functional groups were constrained between 0.85 eV and 1.7 eV. The built-in simplex algorithm in CasaXPS was used to optimize the fitting of functional group peaks to the overall C1s peak with the objective of minimizing the residual. Monte-Carlo simulation was performed to obtain the standard deviations in the calculated peak areas.

Results

The quality and the rate of electroless copper deposition were evaluated using the baseline electroless sensitization and deposition process described in the Experimental Section (i.e. immersion in three sequential baths: (i) tin sensitization bath, (ii) silver activation bath, and (iii) electroless copper deposition bath). The amount of copper deposited onto the epoxy PWBs per area over a 20 min time was obtained gravimetrically, and the results are shown in Figure 1.

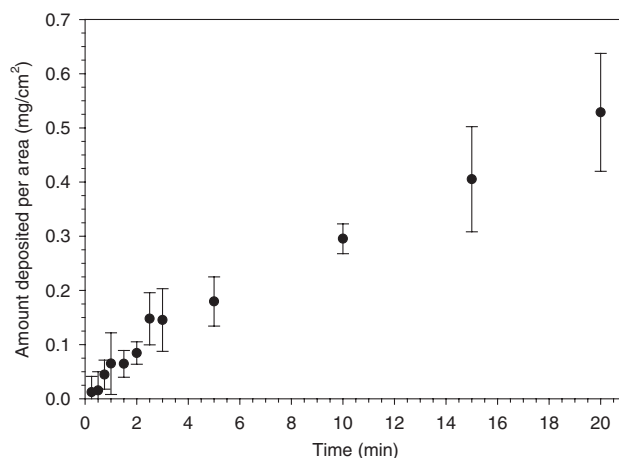


Figure 1. The amount of electroless copper deposited per area on epoxy laminates versus duration of electroless copper deposition.

Four samples were processed to obtain the average mass of copper deposited and the error bars represent the 95% confidence interval. The mass of copper deposited changes almost linearly with time, which implies a constant deposition rate with little induction period needed to initiate deposition. Extrapolation of the longer time experiments back to zero thickness would indicate a 2 to 3 min induction time for the electroless deposition process.⁴² The error during the inductance period is high since there is little copper on the substrate. The average deposition rate calculated from Figure 1 after the induction period is 5.6×10^{-4} mg/cm² s. This deposition rate is in agreement with the deposition rate calculated using mixed potential theory, 6.3×10^{-4} mg/cm² s for this electroless plating bath.¹⁰

One of the interesting aspects of this process is the ability to catalyze the electroless process and achieve acceptable adhesion strength without using a palladium catalyst and the more complicated swell-and-etch pretreatment process. The surface pretreatment step and the catalyst seeding step are two critical steps responsible for the adhesion of electroless copper to the substrate. The conventional swell-and-etch wet-chemical treatment is based on the swelling of the epoxy polymer in a solvent, exposing the oxygen-containing functionalities to the surface and removing them with an etchant.⁸ This method has been shown to increase the surface roughness, which in turn facilitates mechanical anchoring of the seed layer and the subsequent electroless copper layer.

The increase in surface roughness of the PWB substrate resulting from the sulfuric acid treatment was investigated using AFM after 1 min, 30 min and 180 min H₂SO₄ treatments at 95°C. The results were compared to a sample processed by the swell-and-etch treatment. The average (R_a) and root-mean-square (R_q) surface roughness values are shown in Figure 2. The starting PWB material had a R_a surface roughness of 621 nm. There was little change in the surface roughness after 1 min (660 nm), 30 min (685 nm) or 180 min (618 nm), while the swell-and-etch process increased the surface roughness to 819 nm. After 180 min in H₂SO₄, there may have been a degree of surface smoothening due to the removal of the oxygen-containing functionalities.^{8,24}

The evolution of the surface roughness during the electroless copper deposition procedure (sensitization, activation and deposition) was evaluated by AFM also for the tin sensitized, silver activated, electrolessly plated samples (1 and 10 min deposition). The surface roughness values are given in Table I along with the surface roughness values of the starting PWB and the sample treated for 30 min in H₂SO₄. Except for a small increase in roughness as the electroless copper grows in thickness, there is little change in the roughness caused by any of the steps in this silver-catalyzed electroless process. The small decrease in the surface roughness after the silver activation step is possibly due to filling of the valleys in the surface by the Sn/Ag catalyst. The increase in surface roughness in the prolonged electroless copper deposition sample (e.g. 10 min electroless copper deposition sample) can be attributed to the characteristic grainy autocatalytic growth of electroless copper.⁴⁷

The adhesion strength of the deposited electroless copper layer was measured, and the effect of the different sulfuric acid treatment times was evaluated. The adhesion strength values were measured to be 0.40 N/mm for the copper plated sample with 1 min H₂SO₄ treatment, 0.31 N/mm for the copper plated sample with 30 min H₂SO₄ treatment, and 0.33 N/mm for the copper plated sample with 180 min H₂SO₄ treatment. The errors corresponding to a 95% confidence interval were 0.07 N/mm, 0.05 N/mm, and 0.04 N/mm, respectively.

Thus, the H₂SO₄/tin-silver surface treatment was found to produce adherent electroless copper on the PWB substrates without increasing the surface roughness of the starting material. It should be noted that the as-received PWB sample had already some degree of roughness initially, i.e. $R_a = 621$ nm and $R_q = 767$ nm (see Table I). In order to characterize the adhesion strength of smoother samples without changing the sample chemistry, the as-received samples were mechanically polished to decrease their surface roughness, as explained in the Experimental section. The surface roughness values evaluated from the Dektak line scans profilometer were $R_a = 405$ nm and $R_q = 493$

nm before polishing and $R_a = 173$ nm and $R_q = 225$ nm after polishing. A second sample had an initial roughness of $R_a = 430$ nm and $R_q = 531$ nm before polishing, and $R_a = 226$ nm and $R_q = 315$ nm after polishing. The initial surface roughness values found here were less than the values obtained using AFM because the Dektak uses a larger diameter tip than the AFM. The surface roughness values of as-received (i.e. unpolished) samples were slightly different from each other because only one line scan was used to obtain the surface roughness values instead of the more accurate area scans in the AFM measurements. The polished samples were taken through the full H₂SO₄/tin-silver electroless deposition process followed by electroplating copper to build the thickness for adhesion testing. The adhesion strength values of the samples were measured to be 0.032 N/mm and 0.054 N/mm, respectively, for the two samples. This shows that while the H₂SO₄/tin-silver process did not increase the surface roughness, it still depended on the existing roughness to provide some of the adhesion strength.

The atomic composition of the sample surfaces was investigated using XPS survey scans. Table II shows the atomic percentages for a select number of elements at different steps in the electroless process after 0, 10 and 20 s of argon ion etching. The analyzed elements include C, O, Sn, Ag, Cu, S, P, N, and Cl. These elements were selected because they make-up the chemical composition of the epoxy board and involve the species used in the surface pretreatments as well as electroless process. Trace amounts of other elements which do not affect this study, such as silicon and bromine, have been omitted from Table II. The atomic percentages reported in Table II are reported with respect to all the elements found. The results in Table II show the surface and sub-surface elemental composition of the as-received PWB, a PWB taken through the steps of the H₂SO₄/tin-silver process (H₂SO₄ treatment, Sn sensitization, Ag activation and electroless copper deposition), and the samples subjected to surface pretreatments similar to the H₂SO₄ treatment (i.e. the HCl and H₃PO₄ treatments). The sub-surface composition was obtained by ion etching of the sample using an Ar ion gun in the XPS tool. The etch rate of the Ar ion gun was 16.36 nm/s referenced to tantalum. Thus, a 10 s etch corresponds to about 160 nm into the sample, if its etch rate was similar to tantalum.

The as-received epoxy board was mainly composed of carbon (53.69%) and oxygen (24.75%) on the surface, as shown in Table II. The oxygen-to-carbon (O/C) ratio of the as-received sample decreased from 0.46 to 0.08 to 0.05 with depth. Figure 3 shows the surface survey scan for the as-received PWB. Besides carbon and oxygen, small amount of other elements, such as magnesium (0.27%), sodium (1.01%), zinc (1.47%), copper (1.27%), iron (1.24%), chromium (1.81%), nitrogen (2.26%), calcium (0.58%), chlorine (3.63%), sulfur (1.89%), phosphorus (1.45%), silicon (3.68%) and bromine (1.01%) were also identified (not shown in Table II). These are due to additives and other components of the PWB. Silicon comes from the glass fibers in the composite board, and bromine was likely due to flame retardant.⁴³

The hot H₂SO₄ treatment has been identified as an essential step in achieving adherent electroless copper. Omission of the hot sulfuric acid treatment resulted in no electroless copper deposition. Treating the as-received PWB with H₂SO₄ resulted in removal of the trace impurities including magnesium, sodium, zinc, copper, iron, chromium, calcium, chlorine, and phosphorus. The impurities remaining on the PWB were silicon, bromine, nitrogen and sulfur. The increase in the sulfur concentration was a result of the H₂SO₄ treatment. The H₂SO₄ treated sample also shows a decrease in the O/C ratio compared to as-received sample. The O/C ratios going from the surface to the deepest level are 0.32, 0.04, and 0.03, respectively.

The first part of the catalyst seeding was the tin sensitization step. The tin sensitized sample had tin, chlorine, and sulfur in addition to carbon, oxygen, nitrogen, silicon and bromine. Some of the sulfur present on the surface was due to the previous H₂SO₄ treatment. Sn and Cl were likely from the SnCl₂·2H₂O bath used for tin sensitization. The Sn concentration was almost constant at about 7% with depth. The chlorine concentration was also found to remain constant at about 0.8%.

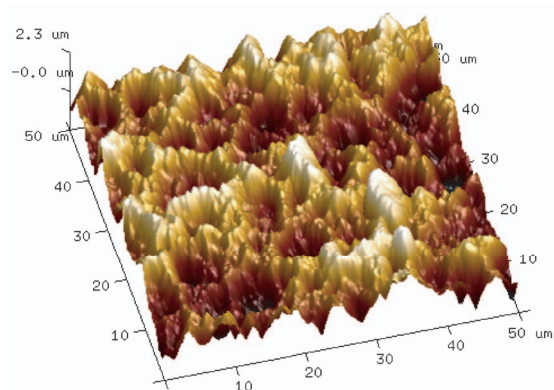
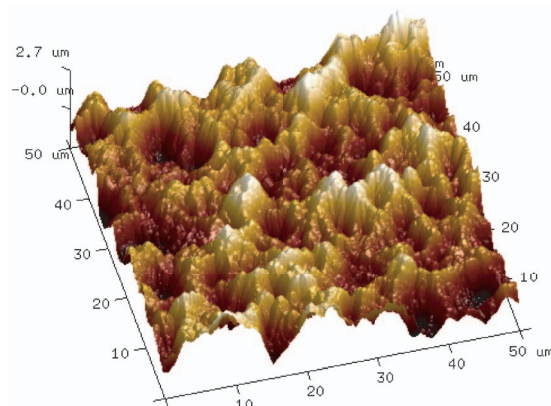
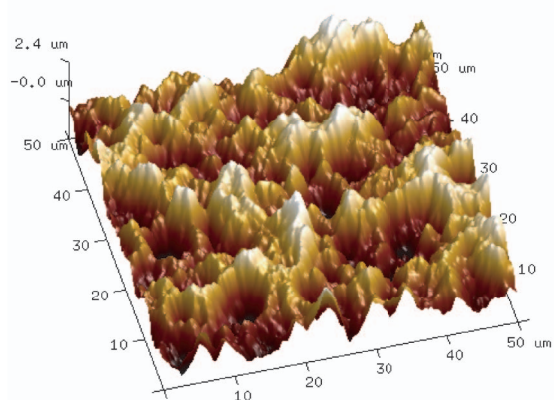
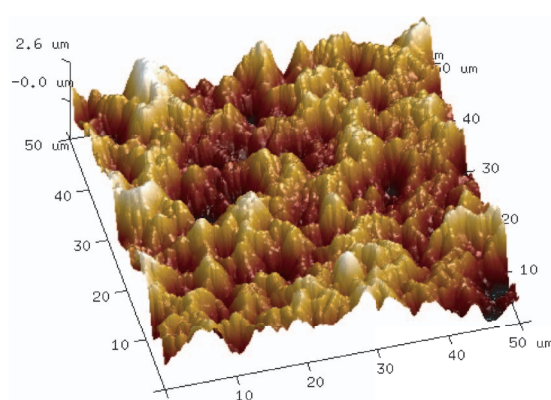
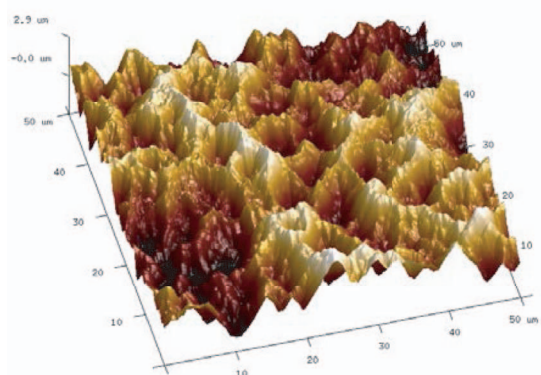
a) Plain Sample, R_a : 621 nm, R_q : 767 nmb) 1 min H_2SO_4 sample, R_a : 660 nm, R_q : 816 nmc) 30 min H_2SO_4 sample, R_a : 685 nm, R_q : 840 nmd) 3 hr H_2SO_4 sample, R_a : 618 nm, R_q : 773 nme) Swell-and-etch sample, R_a : 819 nm, R_q : 997 nm

Figure 2. AFM surface roughness values R_a and R_q obtained for (a) plain epoxy laminate sample, (b) 1 min H_2SO_4 treated sample, (c) 30 min H_2SO_4 treated sample, (d) 3 hr H_2SO_4 treated sample, and (e) swell & etch sample.

The second part of the catalyst seeding procedure involved silver activation after tin sensitization. In the silver activated sample, the elements identified were Ag, Sn, Cl, S, C, O, N, Si and Br. Ag comes from $AgNO_3$ bath. The presence of Sn and Cl is due to Sn sensitization. It was observed that the Ag and Sn concentrations are almost equal to each other at about 2.5% at the surface and the etched sub-surface. A

small increase in the S concentration was observed with depth because of the presence of $(NH_4)_2SO_4$ in the silver activation bath. $AgNO_3$ and $(NH_4)_2SO_4$ in the silver activation bath might also have contributed to the N content.

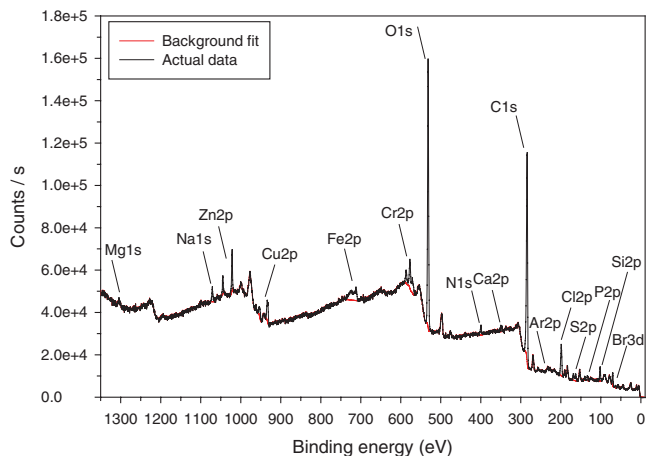
The deposition of electroless copper was performed after the tin sensitization and silver activation steps. The XPS survey scan of the

Table I. The average (R_a) and root-mean-square (R_q) surface roughness values measured for samples at each step in electroless deposition process.

Samples	Surface roughness (nm)	
	R_a	R_q
Plain	621	767
30 min H_2SO_4 treated	685	840
Sn sensitized	691	860
Ag activated	660	808
1 min electroless Cu deposited	660	823
10 min electroless Cu deposited	706	878

copper plated sample shows the presence of Cu, Ag, Sn, Cl, N, C and O. The C and O were likely from adsorbed atmospheric gases onto the copper surface. In addition, a fraction of the O may be due to the oxidation of the electrolessly deposited copper.

The XPS survey scans were taken for the PWB samples exposed to other acids. The H_3PO_4 and HCl treatments were done to see if the copper activation and adhesion was due to simply an acid treatment or if the H_2SO_4 had a more complex role. The elements detected on the HCl treated sample were C, O, Cl, N, Si, and Br. The impurities seen on the as-received sample were completely removed, except Cl. Given the fact the as-received sample also had Cl initially, it was concluded that the Cl content on the HCl treated sample decreased with HCl exposure. The HCl treated sample was taken through the tin sensitization and silver activation process followed by electroless copper plating. However, no electroless copper was deposited on the sample.

**Figure 3.** As-received PWB XPS survey spectrum.

The H_3PO_4 treated sample had an elemental make-up including C, O, P, N, Si and Br. The other impurities were removed. An increase in the P content was observed compared to the as-received sample. The tin sensitization was performed on the H_3PO_4 treated sample. The Sn content on this sample was smaller than that for the sample taken through H_2SO_4 treatment and tin sensitization. The Cl coming from the tin sensitization bath was present in trace amounts. After tin sensitization and silver activation, the H_3PO_4 treated sample was electrolessly copper plated; however, the copper was not uniform in color or thickness on the sample. The resulting surface film was not electrically conductive (i.e. it was not a contiguous film).

Table II. The atomic percentage of elements in samples obtained from XPS survey spectra.

Samples	Etch time (s)	Elements								
		C	O	Sn	Ag	Cu	S	P	N	Cl
Plain	0	53.69	24.75	0.00	0.00	1.27	1.89	1.45	2.26	3.63
	10	79.63	6.38	0.00	0.00	3.02	0.39	0.48	1.28	1.47
	20	83.98	4.36	0.00	0.00	2.24	0.39	0.35	1.08	0.96
H_2SO_4 treated	0	69.65	22.33	0.00	0.00	0.00	3.08	0.00	2.01	0.00
	10	91.32	4.19	0.00	0.00	0.00	1.39	0.00	0.99	0.00
	20	92.30	3.19	0.00	0.00	0.00	1.40	0.00	1.03	0.00
H_2SO_4 treated, Sn sensitized	0	55.40	29.42	7.59	0.00	0.00	2.65	0.00	2.28	0.81
	10	72.28	14.65	7.72	0.00	0.00	1.32	0.00	1.23	0.70
	20	75.40	11.95	6.85	0.00	0.00	1.27	0.00	1.21	0.85
H_2SO_4 treated, Sn sensitized, Ag activated	0	60.73	24.80	2.43	2.67	0.00	3.62	0.00	3.78	0.38
	10	78.04	9.75	2.69	3.02	0.00	1.23	0.00	2.76	0.28
	20	81.25	7.54	2.42	2.68	0.00	1.08	0.00	2.89	0.29
H_2SO_4 treated, Sn sensitized, Ag activated, 6 min Cu deposited	0	17.79	17.51	0.20	0.00	63.79	0.00	0.00	0.00	0.00
	10	5.66	6.38	0.15	0.18	86.98	0.00	0.00	0.00	0.00
	20	11.48	4.70	0.15	0.24	82.45	0.00	0.00	0.20	0.25
HCl treated	0	72.00	20.35	0.00	0.00	0.00	0.00	0.00	2.02	0.77
	10	92.51	3.70	0.00	0.00	0.00	0.00	0.00	0.65	0.35
	20	93.81	2.68	0.00	0.00	0.00	0.00	0.00	0.56	0.45
H_3PO_4 treated	0	57.83	31.08	0.00	0.00	0.00	0.00	7.14	2.04	0.00
	10	88.66	6.31	0.00	0.00	0.00	0.00	2.52	0.81	0.00
	20	90.44	4.65	0.00	0.00	0.00	0.00	2.04	0.99	0.00
H_3PO_4 treated, Sn sensitized	0	77.16	15.70	1.65	0.00	0.00	0.00	1.27	1.33	0.56
	10	91.72	3.20	0.73	0.00	0.00	0.00	1.00	0.80	0.08
	20	92.91	2.22	0.43	0.00	0.00	0.00	0.65	1.33	0.00

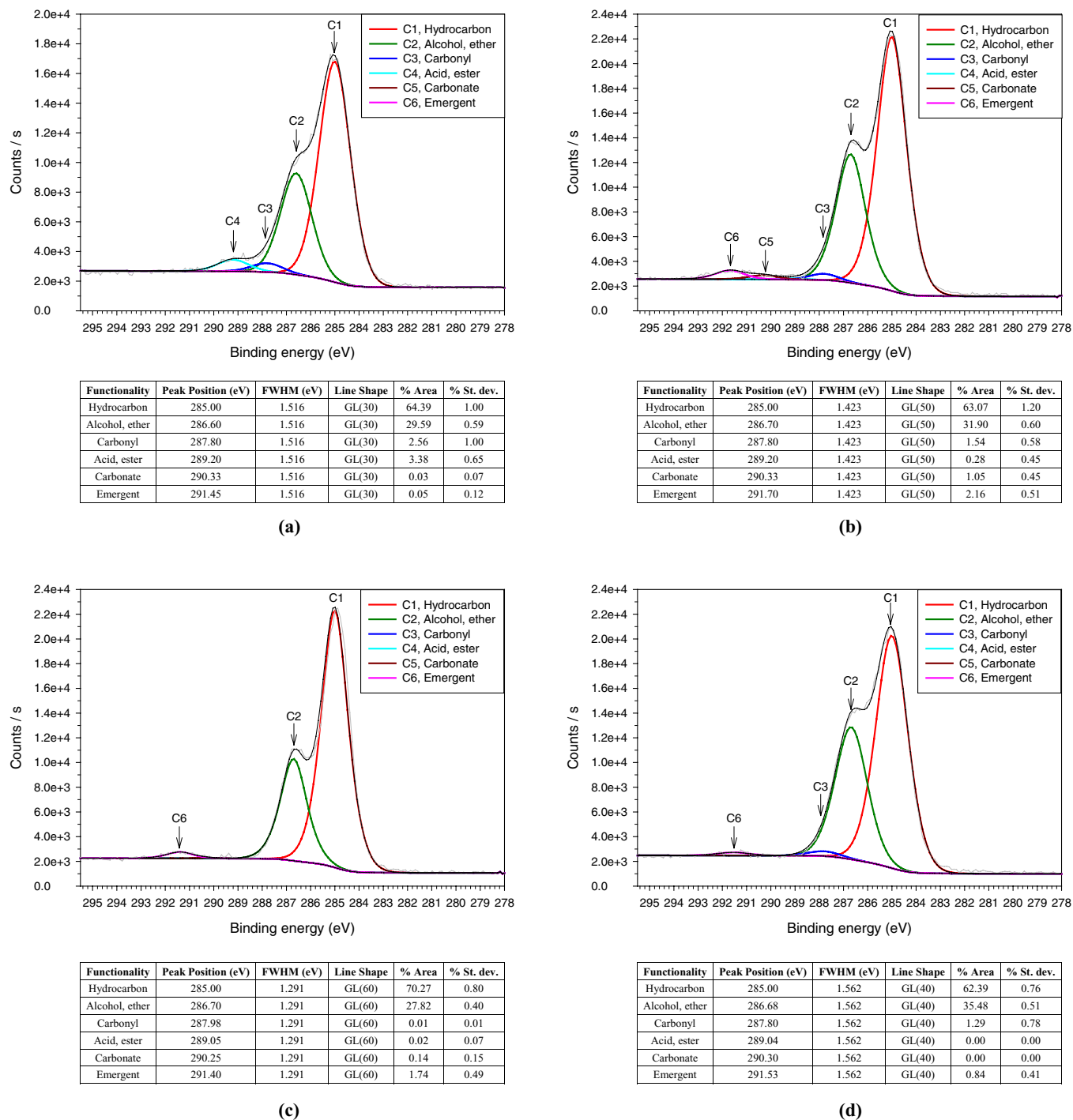


Figure 4. High resolution XPS spectrum, peak fit and peak deconvolution for (a) as-received PWB sample, (b) H₂SO₄ treated PWB sample, (c) H₃PO₄ treated PWB sample, and (d) HCl treated PWB sample.

The XPS survey results shown above characterize the overall elemental composition of the surfaces after each chemical treatment; however, they are limited to simple identification and quantification of the elements present. High resolution elemental XPS analysis of specific elements, such as C1s and O1s, was performed to help understand the detailed changes that occurred on the sample surfaces. The individual elemental peaks were deconvoluted into several peaks corresponding to the different oxidation states or typical chemical functionalities present. In particular, the C1s scan is useful in terms of tracking the change in carbon functional groups as a result of chemical exposure.⁴⁸ Analysis of the O1s peak is less useful than C1s because

oxygen has less of a change in peak position, and because of the presence of adsorbed oxygen on the sample.⁴⁹ It is known that surface treatments affect the outermost sample surface.^{7,8}

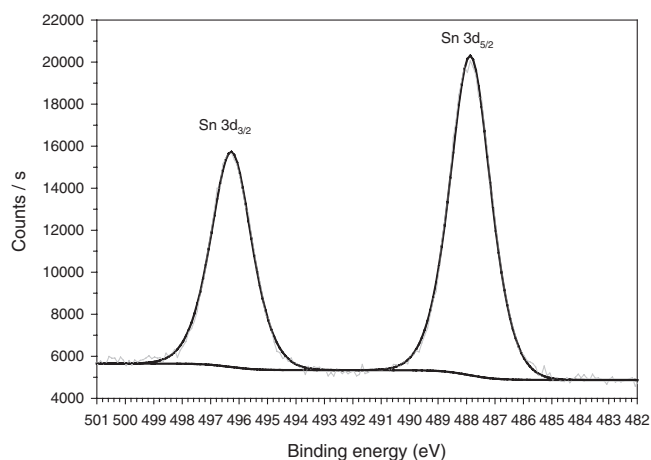
The high resolution surface C1s results are shown in Figure 4. The as-received PWB XPS scan, Figure 4a, can be broken into four different functionalities: 64.39% hydrocarbon-like bonds (C-C, C-H), 29.59% alcohol and ether functionalities (C-O-H, C-O-C), 2.56% carbonyl-like species (C=O), and 3.38% acid and ester-like species (O-C=O). There was no higher oxidation state (i.e. carbonate-like peaks) observed on the as-received sample. After treatment of the as-received PWB in hot H₂SO₄, the molar concentration of

functional groups changed to the following: 63.07% hydrocarbon groups, 31.90% alcohol and ether groups, 1.54% carbonyl groups and 1.05% carbonate groups, as shown in Figure 4b. The fraction identified as acid and ester group was statistically insignificant indicating that the content associated with an acid or ester oxidation state was removed in the hot H_2SO_4 treatment. A second change worth noting after the H_2SO_4 treatment is the emergence of a peak around 291.70 eV, which had a total area of 2.16%. In comparison, the H_3PO_4 treated sample had 70.27% hydrocarbon groups, and 27.82% alcohol and ether groups, as shown in Figure 4c. There was no significant amount of carbonyl, acid and ester, and carbonate species observed on the sample. The peak at 291.40 eV corresponds to 1.74% of the total area. The species identified on the HCl treated sample in Figure 4d are 62.39% hydrocarbon, 35.48% alcohol and ether, and 1.29% carbonyl. There was no carbonate, and acid/ester species found. There was also a new peak observed at 291.53 eV corresponding to 0.84% of the total area. Overall, the amount of carbonyl, and acid/ester functionalities decreased after the acidic surface treatments. The hydrocarbon, and alcohol/ether remained the same or increased slightly, and a new peak at 291.5 eV was observed in all surface treated samples. The XPS spectra after argon ion milling did not show the emergence of this new peak (data is not shown). The peak at 291.5 eV was observed only at the surface of the acid treated samples.

The high resolution XPS scans of tin sensitized and silver activated samples (after a H_2SO_4 treatment) are shown in Figure 5. The spectra were charged shifted holding the C-H, C-C bonds at 285 eV constant. The deconvolution of the peaks was performed using a single deconvolution region and two peak regions (one for each $3d_{5/2}$ and $3d_{3/2}$ peaks) for both tin and silver in order to determine the position and area for each peak. The Gaussian-Lorentzian mixture line shapes were optimized for achieving the minimum residual. Using the same sensitivity factor for the major peaks for each element, the characteristic area ratio of 3:2 for the $3d_{5/2}$ and $3d_{3/2}$ peaks, due to spin-orbit coupling in tin and silver, was found,^{45,46} as shown in Figure 5. The peak positions for the $3d_{5/2}$ and $3d_{3/2}$ peaks corresponded to 487.87 eV and 496.28 eV for tin, and 368.95 eV and 374.94 eV for silver, respectively. Even though it is difficult to distinguish between Sn(II) and Sn(IV) using XPS,⁵⁰ it can be concluded that tin is not in metallic state, i.e. no Sn(0) is present.^{41,51} The literature values reported for binding energy of 487.8 eV coincides mostly with SnO_2 ,^{52–56} although there are some reports for SnO at that binding energy.⁵⁷ It is also possible that Sn may be in the form of a chloride complex.^{51,58,59} The Ag $3d_{5/2}$ peak obtained at 368.95 eV is higher than that reported for elemental silver, 368.2 eV;^{51,60} however the Ag $3d_{5/2}$ peak may be due to elemental Ag^{41,60–62} because the binding energy can differ from bulk values when the metal is in the form of small clusters.⁶⁰ An increase in binding energy has been previously observed for small clusters of Pd, Pt, and Au.^{63,64} The formation of a Sn/Ag alloy could change the binding energy of the Ag $3d_{5/2}$ peak;⁶⁵ however, this appears unlikely due to the lack of a reducing agent for producing Sn from Sn(II). In addition, the formation of a Sn-Ag alloy is not thermodynamically favorable compared to formation of a Sn-Pd alloy in the Pd-based catalysts. The enthalpy of mixing and Gibbs energy of mixing values for Sn-Ag alloy are much less negative than that of Sn-Pd system.⁶⁶ The Sn-Pd binary alloy diagram shows a number of possible crystalline phases at room temperature (Pd_3Sn , Pd_2Sn , Pd_3Sn_2 , PdSn , PdSn_2 , PdSn_3 , PdSn_4). However, the Sn-Ag system does not have a mixed crystalline phase.⁶⁷ The XPS results show that the H_2SO_4 treated sample was indeed seeded with a tin-silver catalyst after the tin sensitization and silver activation steps. It is most likely that the Sn(II) served as the reducing agent for Ag(I) in a way analogous to the tin-palladium catalyst in the traditional Shipley process.¹³

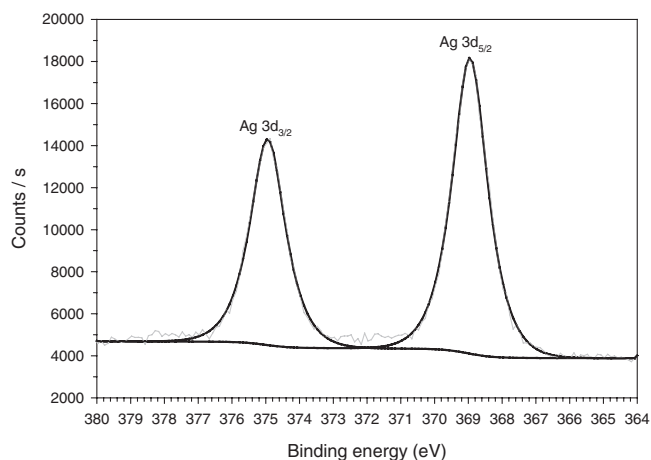
Discussion

The H_2SO_4 pre-treatment has been shown to establish a surface which can be tin sensitized and silver activated. The sensitization and



Peak	Peak Position (eV)	FWHM (eV)	Line Shape	% Area	% St. dev.
Sn $3d_{5/2}$	487.87	1.687	GL(55)	59.77	0.27
Sn $3d_{3/2}$	496.28	1.687	GL(55)	40.23	0.27

(a)



Peak	Peak Position (eV)	FWHM (eV)	Line Shape	% Area	% St. dev.
Ag $3d_{5/2}$	368.95	1.235	GL(80)	58.96	0.30
Ag $3d_{3/2}$	374.94	1.235	GL(80)	41.04	0.30

(b)

Figure 5. Ag activated PWB sample high resolution XPS spectrum, peak fit and peak deconvolution for (a) Sn, and (b) Ag.

activation process forms a colloidal catalyst for the electroless copper deposition. During the catalyst seeding (i.e. tin sensitization and silver activation), Sn(II) is oxidized to Sn(IV), while Ag(I) is reduced to Ag. Silver is a catalyst for the copper formaldehyde electroless bath.^{4,14–16,41}

Seeding of the tin/palladium catalytic colloid onto the epoxy surface is accompanied by an increase in surface roughness in the swell-and-etch process.^{7,8,17,21,24} In contrast, the surface was not appreciably roughened by the H_2SO_4 pretreatment, even for over-treated surfaces, as shown in Figure 2. The results also show that the H_2SO_4 pretreatment produced a unique surface for catalyst seeding, which was not recreated by other strong acids, HCl and H_3PO_4 . There was no or little electroless copper deposited onto the epoxy substrates when other strong acids of similar concentration were used. It was found that times as short as 30 s in H_2SO_4 were adequate to achieving adherent electroless copper deposits on an epoxy substrate. These observations imply that the H_2SO_4 pretreatment is more of chemical change to the surface, rather than simply a mechanical effect, such as increasing the surface roughness.

XPS survey scans give insight into the nature of the H_2SO_4 pretreatment. The as-received sample contained carbon, oxygen, silicon, bromine and nitrogen which are part of the epoxy laminate. The other impurities, including magnesium, sodium, zinc, copper, iron, chromium, calcium, chlorine, and phosphorus were removed by the H_2SO_4 pretreatment. The sulfur concentration increased, due to the presence of sulfate remaining on the sample surface. The replacement of metal ions, most likely in a positive oxidation state, with sulfate anions, may lead to a charge reversal on the epoxy surface which could assist in colloidal adhesion. The effectiveness of even short H_2SO_4 pretreatments shows that only surface changes are taking place. However, simply removing impurities was not sufficient to facilitate catalyst adhesion and electroless copper deposition because the HCl and H_3PO_4 treated surfaces also showed that the impurities were removed from the surface. Only phosphorus remained on the H_3PO_4 treated surface, in addition to the epoxy containing carbon, oxygen, silicon, bromine and nitrogen. The H_2SO_4 and H_3PO_4 pretreatments were similar to the extent that they are both strong acids, removed impurities and left an anion-containing surface. However, the H_3PO_4 pretreatment led to only irregular, trace amounts of electroless copper deposition. The amount of tin detected on the H_3PO_4 pretreated and tin sensitized sample was less than the amount of tin adsorbed on the H_2SO_4 pretreated surface (see Table II). This may be due to the lower solubility for the tin-phosphate complex compared to the tin-sulfate complex.⁶⁸ If the tin precipitates on the surface as the simple salt and not a tin-silver complex, it may be washed away in subsequent washing steps.

In the case of the HCl treated sample, the residual Cl on the surface was less than in the as-received sample. The HCl pretreated sample produced no electroless copper deposition. Thus, it appears that the adsorbed sulfate ions (or small amounts of phosphate ions) enable the colloidal tin ions to be stabilized on the surface during tin sensitization.

Additional information about the chemical effect of the H_2SO_4 pretreatment can be gained from the high resolution surface C1s scans, shown in Figure 4. Apart from removing impurities from the surface and facilitating the sulfate or phosphate adsorption, the nature of the carbon moieties on the surface also can be important. In both the as-received and the acid pretreated samples, the majority of the carbon species, between 94–98%, were from the hydrocarbon (C-C, C-H), and alcohol and ether (C-O-C, C-O-H) groups. There was little or no change in the molar concentration of these functionalities between the as-received sample and those which had been acid pretreated. One common trend observed was a decrease in the carbonyl (C=O), and acid and ester (O-C=O) content after acid treatment, regardless of the acid used. The as-received sample had 2.56% carbonyl species and 3.38% acid and ester species. The concentration of carbonyl, and acid and ester species decreased to 1.54% and 0.28% after H_2SO_4 pretreatment, 0.01% and 0.02% after H_3PO_4 pre-treatment, and 1.29% and 0.00% after HCl treatments, respectively. It is possible that the strong acids attack the carbonyl oxygens due to their Lewis base nature (i.e. electron pair donor). This acid-base interaction can lead to bond breaking and formation of CO and CO_2 .^{27,35} This is also reflected in the decrease in surface O/C ratio for the acid treated samples. The as-received sample had a O/C ratio of 0.46 whereas the H_2SO_4 pretreated sample had a surface ratio of 0.32 and the HCl sample had a value of 0.28. The H_3PO_4 pretreated sample did show an increase in the O/C ratio, possibly due the high oxygen content in the phosphate. It is noted that strong acids can oxidize the carbonyl, acid and ester species to a higher oxidation state, such as carbonate.^{27,35}

An interesting difference in C1s scans between the as-received and acid treated samples is the occurrence of a new peak at 291.5 eV, Figure 4. This new peak was found only at the surface and not in the argon ion etched scans. This peak may be due to newly formed CO_2 or CO upon bond breaking by acid treatment.^{69–71} It is known that the surface pre-treatment mostly affects the surface and not the sub-surface.⁸

The colloidal nature of the tin sensitized and silver activated surface can be seen in the $\text{Sn } 3d_{5/2}$ peak at 487.87 eV with a spin-orbit splitting of 8.41 eV. This binding energy indicates that no elemental

Sn is present^{41,51} (i.e. Sn is found to be either in Sn(II) or Sn(IV) form).^{52–57} The tin is more likely in the Sn(IV) form as in SnO_2 .^{52–56} The binding energy for Sn is also in accordance with a Sn chloride complexes.^{51,58,59} Even though the observed binding energy of 368.95 eV for $\text{Ag } 3d_{5/2}$ peak is slightly higher than the reported value of 368.2 eV in the literature,^{51,60} it is likely that this increase is due to Ag being packed in small clusters,⁶⁰ and Ag was most probably in elemental state.^{41,60–62} These findings support the reduction of Ag(I) to Ag(0) by oxidation of Sn(II) to Sn(IV) .^{14,15,41} It appears that the most likely form of the tin-silver species is as a core-shell nano-colloid which has a metallic silver core surrounded by a Sn(IV) species, which are likely to be SnO_2 and/or a tin-chloride complex. The possibility of the tin being in a tin-chloride complex is consistent with the high concentration of Cl in the XPS spectra, Table II. The negatively charged Cl^- ions may serve as a stabilizer for the nano-colloid.^{11,12,15,16}

The XPS survey results for the H_2SO_4 pretreated sample after tin sensitization and silver activation showed almost a 1:1 atomic concentration ratio for the Sn and Ag . In our two-step catalyst seeding process, the concentration of Ag in the Ag bath, 22.1 mM, was less than the concentration of Sn in the Sn bath, 36.6 mM. Similarly, in the study by Fujiwara et al., the nano-colloids showed approximately a 1:1 Sn:Ag atomic ratio (see “not conditioned” curve in Figure 4 in Ref. 15), even though the catalyst seeding solution had 10 mM Ag and 100 mM Sn . These results indicate that Ag is likely the limiting reagent in the nano-colloid formation. This is supported by the study of Vaskelis et al. where an increase in the density of the Sn/Ag colloid was observed by UV-vis spectroscopy when the Ag(I) concentration was increased in the presence of excess Sn(II) .¹⁴ The 1:1 atomic ratio observed in this study and also in the study by Fujiwara et al.,¹⁵ indicates that all the Ag(I) which was reduced by the Sn(II) oxidation does not end up in the nano-colloid because then the Sn:Ag ratio would be 1:2. Alternatively, the Sn(II) could reduce another species, in addition to Ag(I) resulting in a Sn:Ag ratio of about 1:1.

Finally, the findings reported here can be used to summarize the mechanism for the adhesion of the electroless copper onto the epoxy laminate substrates. The H_2SO_4 treatment ultimately improves the copper adhesion and facilitates the adsorption of the Sn/Ag catalyst without increasing the surface roughness. Impurities were removed from the as-received substrate in the H_2SO_4 pretreatment leading to a charge reversal on the surface. The number of carbonyl, acid and ester functionalities gets decreased. In addition, the lower O/C ratio shows that the carbonyl surface was changed. The H_2SO_4 pretreated surface had adsorbed sulfate ions which enabled Sn(II) sensitization. Ag activation occurred through reduction of the Ag(I) forming a core-shell nano-colloid. The nano-colloids are likely negatively charged due to the presence of the chloride complexing agent. This negative charge can prevent the agglomeration of the nano-colloids. The electrochemical reaction involving reduction of Cu(II) to Cu(0) and oxidation of formaldehyde is catalyzed by the Sn/Ag nano-colloids leading to adherent, continuous and uniform electroless copper deposition on the epoxy laminate substrates.

Conclusions

In this study, electroless copper plating on epoxy laminates has been investigated using a Ag -based catalyst, and non-roughening sulfuric acid surface treatment. Conventional Pd -based catalyst is expensive, and the widely used swell-and-etch method creates substantial surface roughness which is detrimental for electrical performance. The H_2SO_4 treatment was observed to introduce little or no surface roughness to the epoxy laminate. No electroless copper deposition was observed without the H_2SO_4 treatment. The amount of carbonyl (C=O) and acid/ester (O-C=O) functionalities were observed to decrease after the H_2SO_4 treatment. Surface pretreatment with H_2SO_4 was unique in catalyst seeding, compared to other acid treatments including HCl and H_3PO_4 . The sulfate content adsorbed on the epoxy laminate after H_2SO_4 treatment enabled Sn(II) sensitization by electrostatic attraction. XPS results indicated Sn(II) oxidation to Sn(IV)

and Ag(I) reduction to Ag(0), so as to form a core-shell nano-colloidal catalyst with Ag(0) core and SnO₂ shell. It is possible that some SnCl₃⁻ resided on the outer surface of the nano-colloids providing stability by preventing agglomeration.^{11,12} Sn/Ag nano-colloids were observed to catalyze the electroless copper deposition. Overall, the chemical adhesion was promoted by H₂SO₄ treatment rather than mechanical adhesion, and the use of Sn/Ag catalyst with H₂SO₄ surface treatment facilitated adherent, continuous and uniform electroless copper layers on epoxy laminates.

References

1. E. J. O'Sullivan, in *Advances in Electrochemical Science and Engineering, Volume 7*, p. 225, Wiley-VCH Verlag GmbH (2001).
2. C. P. L. Li, P. Ciccolo, and D. K. W. Yee, *Circuit World*, **36**, 31 (2010).
3. M. Paunovic, in *Modern Electroplating*, p. 433, John Wiley & Sons, Inc. (2010).
4. N. Fritz, H. Koo, Z. Wilson, E. Uzunlar, Z. Wen, X. Yeow, S. Allen, and P. Kohl, *J. Electrochem. Soc.*, **159**, D386 (2012).
5. E. J. Denlinger, *IEEE Trans. Microw. Theory Tech.*, **28**, 513 (1980).
6. N. A. Z. Zakaria and C. Free, in *RF and Microwave Conference, RFM 2004 Proceedings*, p. 93, Selangor, Malaysia (2004).
7. S. Siau, A. Vervaet, E. Schacht, and A. Van Calster, *J. Electrochem. Soc.*, **151**, C133 (2004).
8. S. Siau, A. Vervaet, L. Van Vaec, E. Schacht, U. Demeter, and A. Van Calster, *J. Electrochem. Soc.*, **152**, C442 (2005).
9. I. Ohno, O. Wakabayashi, and S. Haruyama, *J. Electrochem. Soc.*, **132**, 2323 (1985).
10. M. Paunovic and M. Schlesinger, *Fundamentals of Electrochemical Deposition*, p. 144, Wiley, New York (1998).
11. O. Holderer, T. Epicier, C. Esnouf, and G. Fuchs, *Journal of Physical Chemistry B*, **107**, 1723 (2003).
12. R. L. Cohen and K. W. West, *J. Electrochem. Soc.*, **120**, 502 (1973).
13. C. R. Shipley, U.S. Patent, 3,011,920 (1961).
14. A. Vaskelis, A. Jagminiene, L. Tamasauskaitė-Tamasiunaite, and R. Juskenas, *Electrochim. Acta*, **50**, 4586 (2005).
15. Y. Fujiwara, Y. Kobayashi, K. Kita, R. Kakehashi, M. Noro, J. Katayama, and K. Otsuka, *J. Electrochem. Soc.*, **155**, D377 (2008).
16. Y. Fujiwara, Y. Kobayashi, T. Sugaya, A. Koishikawa, Y. Hoshiyama, and H. Miyake, *J. Electrochem. Soc.*, **157**, D211 (2010).
17. S. Siau, A. Vervaet, A. Van Calster, I. Swennen, and E. Schacht, *J. Electrochem. Soc.*, **151**, J54 (2004).
18. A. Pizzi and K. L. Mittal, *Handbook of Adhesive Technology*, 2nd ed., p. 53, Marcel Dekker, Inc., New York, U.S.A. (2003).
19. S. Ebnasajjad, *Surface Treatment of Materials for Adhesion Bonding*, p. 77, William Andrew Pub., Norwich, NY, U.S.A. (2006).
20. S. Siau, A. Vervaet, E. Schacht, U. Demeter, and A. Van Calster, *Thin Solid Films*, **495**, 348 (2006).
21. S. Siau, A. Vervaet, E. Schacht, S. Degrande, K. Callewaert, and A. Van Calster, *J. Electrochem. Soc.*, **152**, D136 (2005).
22. J. Ge, R. Tuominen, and J. K. Kivilahti, *Journal of Adhesion Science and Technology*, **15**, 1133 (2001).
23. J. Ge, M. P. K. Turunen, and J. K. Kivilahti, *Thin Solid Films*, **440**, 198 (2003).
24. D. Schroer, R. J. Nichols, and H. Meyer, *Electrochim. Acta*, **40**, 1487 (1995).
25. S. Siau, A. Vervaet, S. Nalines, E. Schacht, and A. Van Calster, *J. Electrochem. Soc.*, **151**, C816 (2004).
26. T. Laine-Ma, P. Ruuskanen, S. Kortet, and M. Karttunen, *Circuit World*, **35**, 22 (2009).
27. J. Ge, M. P. K. Turunen, M. Kusevic, and J. K. Kivilahti, *Journal of Materials Research*, **18**, 2697 (2003).
28. S. Siau, A. Vervaet, S. Nalines, E. Schacht, and A. Van Calster, *J. Electrochem. Soc.*, **151**, C831 (2004).
29. S. Asakura, S. Fukutani, and A. Fuwa, *Microelectron. Eng.*, **75**, 375 (2004).
30. D. Schaubroeck, J. De Baets, T. Desmet, P. Dubrue, E. Schacht, L. Van Vaec, and A. Van Calster, *Appl. Surf. Sci.*, **256**, 6269 (2010).
31. D. Schaubroeck, E. Van Den Eeckhout, J. De Baets, P. Dubrue, L. Van Vaec, and A. Van Calster, *Journal of Adhesion Science and Technology*, **26**, 2301 (2012).
32. B. Mkhlef, A. Copley, L. Paniwnyk, and T. Mason, *Circuit World*, **38**, 124 (2012).
33. A. Copley and T. Mason, *Circuit World*, **34**, 18 (2008).
34. G. G. Kim, J. A. Kang, J. H. Kim, S. J. Kim, and N. H. Lee, *Surface & Coatings Technology*, **201**, 3761 (2006).
35. J. Ge, M. P. K. Turunen, and J. K. Kivilahti, *J. Polym. Sci. Pt. B-Polym. Phys.*, **41**, 623 (2003).
36. H. Hayden, E. Elce, S. A. B. Allen, and P. A. Kohl, *IEEE Trans. Adv. Packag.*, **32**, 758 (2009).
37. E. Sheng, I. Sutherland, D. M. Brewis, and R. J. Heath, *Journal of Adhesion Science and Technology*, **9**, 47 (1995).
38. F. P. M. Mercx, A. Benzina, A. D. Vanlangveld, and P. J. Lemstra, *Journal of Materials Science*, **28**, 753 (1993).
39. <http://hazard.com/msds/mf/baker/baker/files/p5719.htm>.
40. <http://www.isola-group.com/products/185hr/>.
41. Y. Kobayashi, V. Salgueirino-Maceira, and L. M. Liz-Marzan, *Chemistry of Materials*, **13**, 1630 (2001).
42. M. Schlesinger and M. Paunovic, *Modern electroplating*, p. 645, John Wiley, New York (2000).
43. M. W. Jawitz, *Printed circuit board materials handbook*, p. 6.3, McGraw-Hill, New York (1997).
44. <http://www.thermoscientific.com/surfaceanalysis>.
45. <http://www.casaxps.com/>.
46. J. C. Vickerman, *Surface Analysis: The Principal Techniques*, p. 56, 2nd ed., John Wiley, Chichester, UK (1997).
47. R. Sard, *J. Electrochem. Soc.*, **117**, 864 (1970).
48. D. Briggs, *Surface analysis of polymers by XPS and static SIMS*, p. 67, Cambridge University Press, New York, U.S.A. (1998).
49. E. I. Yasuda, M. Inagaki, K. Kaneko, M. Endo, A. Oya, and Y. Tanabe, *Carbon Alloys: Novel Concepts to Develop Carbon Science and Technology*, p. 216, Elsevier Science Ltd, Oxford, UK (2003).
50. G. Alonzo, N. Bertazzi, J. R. Ferraro, A. Furlani, G. Iucci, G. Polzonetti, and M. V. Russo, *Appl. Spectrosc.*, **49**, 237 (1995).
51. NIST X-ray Photoelectron Spectroscopy Database <http://srdata.nist.gov/xps/>.
52. J. Pla, M. Tamasi, R. Rizzoli, M. Losurdo, E. Centurioni, C. Summonte, and F. Rubinelli, *Thin Solid Films*, **425**, 185 (2003).
53. F. H. Li, J. X. Song, F. Li, X. D. Wang, Q. X. Zhang, D. X. Han, A. Ivaska, and L. Niu, *Biosensors and Bioelectronics*, **25**, 883 (2009).
54. B. Mirkelamoglu and G. Karakas, *Applied Catalysis a-General*, **299**, 84 (2006).
55. Z. B. Zhou, R. Q. Cui, G. M. Hadi, W. Y. Li, and Z. M. Ding, *Journal of Materials Science-Materials in Electronics*, **12**, 417 (2001).
56. A. Lewera, P. J. Barczuk, K. Skorupska, K. Miecznikowski, M. Salamoneczyk, and P. J. Kulesza, *Journal of Electroanalytical Chemistry*, **662**, 93 (2011).
57. M. Mancini, P. Kubiak, M. Wohlfahrt-Mehrens, and R. Marassi, *J. Electrochem. Soc.*, **157**, A164 (2010).
58. S. A. Bocanegra, A. Guerrero-Ruiz, S. R. de Miguel, and O. A. Scelza, *Applied Catalysis a-General*, **277**, 11 (2004).
59. A. Sharma, G. Andersson, and D. A. Lewis, *Physical Chemistry Chemical Physics*, **13**, 4381 (2011).
60. L. J. Zhi, T. Zhao, and Y. Z. Yu, *Scripta Materialia*, **47**, 875 (2002).
61. R. Adhikari, G. Gyawali, T. Sekino, and S. W. Lee, *Journal of Solid State Chemistry*, **197**, 560 (2013).
62. S. M. Lee, H. J. Cho, J. Y. Han, H. J. Yoon, K. H. Lee, D. H. Jeong, and Y. S. Lee, *Materials Research Bulletin*, **48**, 1523 (2013).
63. M. G. Mason, *Phys. Rev. B*, **27**, 748 (1983).
64. G. K. Wertheim, S. B. Diczio, and S. E. Youngquist, *Physical Review Letters*, **51**, 2310 (1983).
65. K. Santhi, E. Thirumal, S. N. Karthick, H. J. Kim, M. Nidhin, V. Narayanan, and A. Stephen, *Journal of Nanoparticle Research*, **14**, 12 (2012).
66. R. Hultgren, P. D. Desai, D. T. Hawkins, M. Gleiser, and K. K. Kelley, *Selected Values of the Thermodynamic Properties of Binary Alloys*, p. 103, American Society for Metals, Ohio (1973).
67. *ASM Handbook, Volume 3*, ASM International, Ohio (1992).
68. *CRC Handbook of Chemistry and Physics*, p. B140, 69th ed, CRC Press, Inc., Florida, U.S.A. (1977).
69. J. Knudsen, N. M. Martin, E. Granas, S. Blomberg, J. Gustafson, J. N. Andersen, E. Lundgren, S. Klacar, A. Hellman, and H. Gronbeck, *Phys. Rev. B*, **84**, 6 (2011).
70. T. E. Felter, W. H. Weinberg, G. Y. Lastushkina, A. I. Boronin, P. A. Zhdan, G. K. Borek, and J. Hrbek, *Surface Science*, **118**, 369 (1982).
71. M. W. Abee, Interaction of Acid/Base Probe Molecules with Specific Features on Well-Defined Metal Oxide Single-Crystal Surfaces, in *Chemical Engineering Department*, p. 141, Doctor of Philosophy Thesis, Virginia Polytechnic Institute and State University (2001).